

PCCP

Accepted Manuscript



This is an *Accepted Manuscript*, which has been through the Royal Society of Chemistry peer review process and has been accepted for publication.

Accepted Manuscripts are published online shortly after acceptance, before technical editing, formatting and proof reading. Using this free service, authors can make their results available to the community, in citable form, before we publish the edited article. We will replace this *Accepted Manuscript* with the edited and formatted *Advance Article* as soon as it is available.

You can find more information about *Accepted Manuscripts* in the [Information for Authors](#).

Please note that technical editing may introduce minor changes to the text and/or graphics, which may alter content. The journal's standard [Terms & Conditions](#) and the [Ethical guidelines](#) still apply. In no event shall the Royal Society of Chemistry be held responsible for any errors or omissions in this *Accepted Manuscript* or any consequences arising from the use of any information it contains.

ARTICLE

Novel porphyrins-preparation, characterization, and application in solar energy conversion

Cite this: DOI: 10.1039/x0xx00000x

Jianfeng Lu,^{‡a} Hao Li,^{‡a} Shuangshuang Liu,^a Yu-Cheng Chang^b, Hui-Ping Wu^b, Yibing Cheng^{a,c}, Eric Wei-Guang Diau^{b*} and Mingkui Wang^{a*}Received 00th January 2012,
Accepted 00th January 2012

DOI: 10.1039/x0xx00000x

www.rsc.org/

Porphyrins have been demonstrated as one of most efficient sensitizers in dye-sensitized solar cells (DSSC). Herein, we investigated a series of porphyrin sensitizers functionalized with various π -spacers, such as phenyl for LD14, thiophene for LW4, thiophene-phenyl for LW5, and 2,1,3-benzothiadiazole (BTD)-phenyl for LW24. Photo-physical investigation by means of time-resolved fluorescence and nanosecond transient absorption spectroscopy revealed an accelerated inner charge transfer in porphyrin containing the BTD-phenyl π -spacer. Implementing of an auxiliary electron-deficient BTD unit to the porphyrin spacer also results in a broad light-harvesting ability extended up to 840 nm, contributing from an enhanced charge transfer character from porphyrin ring to the anchoring group. When utilized as a sensitizer in DSSC, the LW24 device achieved the power conversion efficiency of 9.2%, higher than those based on LD14 or LW5 porphyrins (PCE 9.0% or 8.2%, respectively) but lower than the LW4 device (PCE 9.5%). Measurements of transient photovoltage decays demonstrate that the LW24 device features the up-shifted potential band edge of the conduction band of TiO₂, but involves serious charge recombination in the dye/TiO₂ interface. The findings provide insight between the molecular structure and the charge-transfer characteristics for designing of efficient porphyrin sensitizers for DSSC applications.

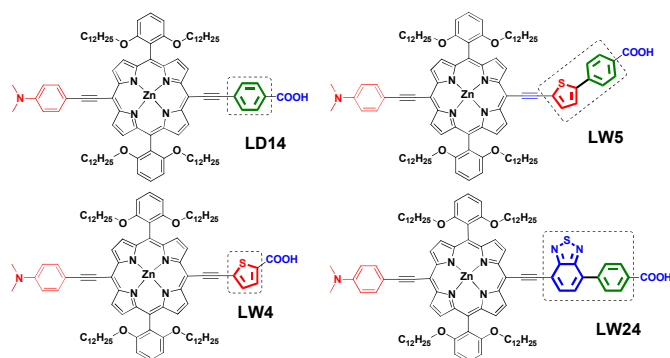
Introduction

Emulation of photosynthesis and efficient and sustainable utilization of solar energy have become one of the greatest scientific challenges in the 21st century. Porphyrins and their derivatives play vital role in photosynthesis due to their superior light-harvesting ability in the visible spectrum, easy tuning photo- and electrochemistry through functionalization of the periphery (meso and β -positions) as well as variation of the metal centre.¹ In addition to this, these properties lead to fruitful optoelectronic application, such as molecular electronics, solar cells, hydrogen evolution, and so on.² Synthetic porphyrin are widely incorporated in prototype dye-sensitized solar cells (DSSC), in which specifically rational designed porphyrin sensitizers have afforded top power conversion efficiency (PCE), outperforming the standard Ru-polypyridyl dyes.³ Most of highly efficient porphyrin sensitizers have a feature of donor-acceptor conjunction.⁴ However, typical D-A porphyrin sensitizers has intense but sharp light absorption in the B (450 nm) and Q (550-650 nm) bands, bereft of absorption around 500-600 nm and beyond 750 nm. In pursuit of panchromatic porphyrin sensitizers, extensive attention has been paid on modification of the donor and acceptor structure for D-A porphyrins, resulting in variations in optical and photovoltaic property.⁵ Notably, elongation of π conjugation and loss of symmetry in porphyrin molecules have been recognized to

broaden and red shift their absorption bands.^{2a} Detailed investigation has showed that porphyrin's optoelectronic property could be efficiently modulated by adjusting the electronic unit between porphyrin core and anchor.⁶ This particular unit is termed as the conjugating 'spacer' in this study as discussed below. The progress of porphyrin applications in DSSC over the past few years has evidenced the large contribution from a rational design of spacer groups, including the DSSC PCE record of 13.0% from porphyrin SM315, which incorporates a new spacer by implementing an auxiliary electron-deficient unit of benzothiadiazole (BTD) into phenyl spacer.^{3c} However, it is worthy to note the DSSC PCE dramatically decreased to 2.5% if the spacer was changed from BTD-phenyl to BTD.⁷ Furthermore, Palomares *et al.* reported that only a tiny change of single atom in spacer could play big influence on porphyrins property. They found that the DSSC efficiency can be largely improved from 2.55% to 10.41% by changing BTD-furan to BTD-thiophene.⁸ These results expose the crucial role of spacer's structure in porphyrin sensitizers. Therefore, a modification at the spacer is expected to induce significant effect on the porphyrin sensitizers' optical, redox, and their photovoltaic properties, suggesting a feasible choice rather than on the donor to modulate the optoelectronic properties of porphyrin sensitizers.^{3c-3e, 7-8} Following this strategy, a bunch of porphyrin sensitizers were developed for DSSC, showing over 10% PCE.^{3d,3e} It is also worth to note that a

same group could have distinct different effect on porphyrin's spectral and photovoltaic properties when placed at different positions, such as donor or acceptor moieties (i.e., two different *meso*-positions). For example, Officer and Gordon demonstrated that the acceptor moiety, which act as a bridge between the porphyrin and the oxide semiconductor surface, have stronger interaction with the macrocycle than the donor moiety in such D-A type porphyrins.⁹ Wang *et al* reported that the DSSC performance could be improved by 50% when placing electron-deficient unit 2,3-diphenylquinoxaline (DPQ) at the acceptor moiety rather than at donor moiety.¹⁰ On the other hand, there are also extensive work on aryl-ethynyl substituted tetrapyrroles, showing variations in optical and redox properties with variations in the aryl group attached to an ethynyl. For example, by attaching additional potent auxochromes to the donor *meso*-positions, Lin *et al* also reported highly efficient porphyrin sensitizers covering Near-IR region.¹¹ We notice that few studies have been done on relationship between device property and porphyrin structure through analysis of the photo-induced charge transfer *via* spacers.

Due to the importance of spacer in porphyrins, we have tested various spacers in D-A structured sensitizers. Consequently, we found that by changing spacer unit from phenyl to thiophene, the devices PCEs could be improved from 9.0% to 9.5%.¹² Therein, thiophene is an electron-rich unit while BTD is electron-deficient unit. A question still opens about the effect of conjugating spacer units on photo-induced charge transfer in porphyrins. In this article, we report our finding on the conjugating spacer group to the terminal benzoic acid group that is the determinant in the variations in optical, redox of porphyrins. Four D-A type porphyrin sensitizers differentiated in the conjugating spacers, *i.e.* phenyl (LD14),¹³ thiophene (LW4), thiophene-phenyl (LW5) or BTD-phenyl (LW24), were investigated. The selected spacer units possess electron-deficient or rich properties, thus providing significant information to rational design highly efficient porphyrin sensitizers. We found that with a solely aromatic spacer in these porphyrins, the resulted DSSC presents an improved performance due to an increasing of electron-donating ability from phenyl to thiophene. The electron deficient aromatic BTD shows more beneficial than electron-rich thiophene as a spacer extending unit.

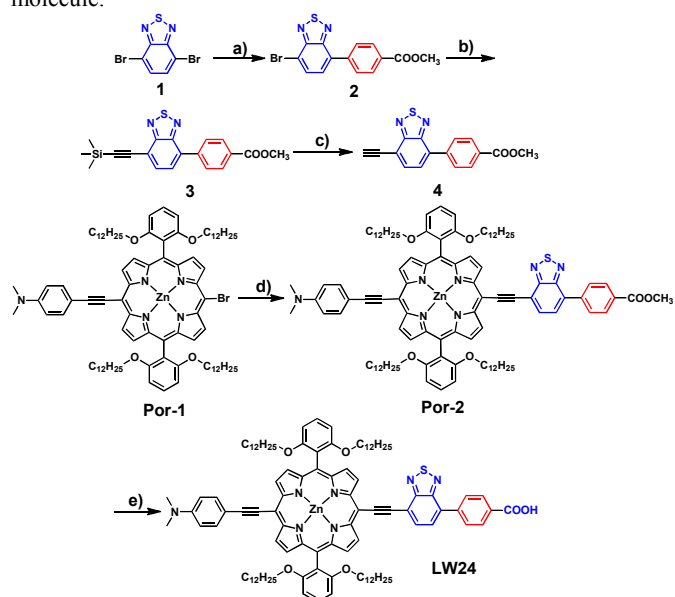


Scheme 1. Molecular structure of the porphyrins LW4, LW5, LW24 and LD14.

Result and Discussion

The molecular structures of porphyrin LD14, LW4, LW5, and LW24 are presented in Scheme 1. Rigid anchor structure and long alkoxy chain are designed to reduce the recombination reaction induced by molecule aggregation. As shown in Scheme 1, the only difference for the four porphyrins structures is the spacer moiety, aiming to make a clear comparison of spacers for porphyrins. The LD14 with phenyl and LW4 with thiophene are supposed to study the influence of spacer's electron-donating ability on optoelectronic properties of porphyrins and their photovoltaic devices. While the LW5 and LW24 dyes are designed to determinate whether an electron-deficient or rich aromatic as a spacer extender is more suitable for DSSC.

The synthesis of LW24 is summarized in Scheme 2. Unlike the synthesis approach for SM315 or LCVC-series porphyrins as reported by Grätzel and Palomares,^{3c,7-8} we introduced pre-synthesized acceptors to porphyrin at the last step, which has been demonstrated to be an efficient and high purity ensured method.¹⁴ Firstly, the 4,7-dibromobenzo[c][1,2,5] thiadiazole (compound **1**) was coupled with (4-methoxyphenyl) boronic acid *via* Pd-catalyzed Suzuki coupling reaction. Then, treating the compound **2** with trimethylsilylacetylene, Pd-catalyzed Sonogashira coupling reaction was carried out to obtain compound **3**. Later on, compound **4** was achieved in the K_2CO_3 /MeOH alkalescence environment. Finally, a standard Sonogashira cross-coupling reaction was applied to synthesize the D-A structured **Por-2**, which was further treated with sodium hydroxide and diluted hydrochloric acid to get final target molecule.



Scheme 2. Synthesis of the LW24 porphyrins: a) **1**, (4-methoxyphenyl) boronic acid, $Pd(PPh_3)_4$, THF, 2 M K_2CO_3 , reflux, overnight; b) **2**, TMSA, $Pd(OAc)_2$, PPh_3 , CuI, THF/TEA, 45 °C, 24 h; c) **2**, K_2CO_3 , MeOH, room temperature, 6 h; d) **Por-1**, **4**, $Pd(PPh_3)_4$ /CuI, THF/TEA, 45 °C, 18 h; e) i) **Por-2**, 20% NaOH(aq.), THF, 40 °C, 2 h; ii) diluted HCl.

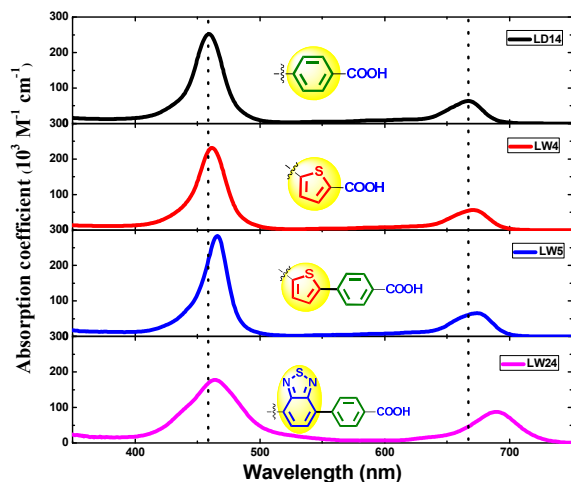


Fig. 1 The absorption spectra of LD14, LW4, LW5, and LW24. All measurements were done in 4×10^{-6} mol/L in THF solution at 25 °C.

The absorption spectra of these porphyrin dyes are shown in Fig. 1 and corresponding data are tabulated in Table 1. The resulted dyes exhibit two typical porphyrin B and Q absorption band at 450-570 and 650-750 nm. The former band involves the transition from the ground state to the second excited state ($S_0 \rightarrow S_2$), while the latter stems from the weaker transition to the first excited state ($S_0 \rightarrow S_1$).^{3c} As depicted in Fig. 2a, the Q band of the LW4 is slightly red-shift by 4 nm comparing to the LD14, causing from the spacer substitution from phenyl to thiophene. For the thiophene-phenyl conjugated LW5, the Q-band red-shifts about 3 nm compared to that of LW4. Indeed, elongation of π conjugation and loss of symmetry in porphyrin molecule result in broadened and red shifted absorption bands.^{2a} Thus, we can ascribe the red-shift of LW4 (compared to LD14) to the latter reason, while the LW5 (compared with LD14 or LW4) to the former. When replacing thiophene (an electron-rich unit) with BTD (an electron-deficient aromatic unit), the Q band dramatic red-shifts by 15 nm from 674 nm for porphyrin LW5 to 689 nm for porphyrin LW24, as presented in Fig. 2b. Otherwise, the Q band maximum molar extinction coefficient of LW24 increases 30% to $8.8 \times 10^4 \text{ M}^{-1} \text{ cm}^{-1}$ comparing to LW5 ($6.6 \times 10^4 \text{ M}^{-1} \text{ cm}^{-1}$), indicating a promising application for thin-film DSSCs.^{12e} Since the conjugation length of LW5 and LW24 are very similar, the above results suggest that the porphyrin dye's absorption spectrum greatly dependant on the intrinsic property of the spacer unit. It also means that a versatile synthesis platform for panchromatic porphyrin could be expected by adjusting the aromatics in the spacer part.

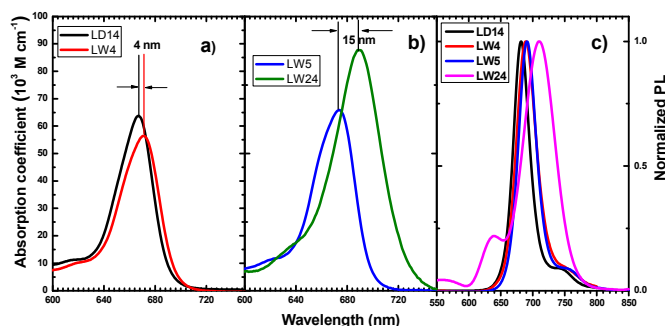


Fig. 2 a) The Q band absorption spectra of LW4 and LD14; b) The Q band absorption spectra of LW5 and LW24; c) The steady-state emission of LD14 LW4, LW5, and LW24. All measurements were done with 4×10^{-6} mol/L THF solution at 25 °C.

The fluorescent emission maxima of LD14, LW4, LW5 and LW24 dyes in THF solution are found at 684, 687, 691, and 710 nm, showing mirror image to their Q absorption bands as depicted in Fig. 2c. The increased Stokes shift of the LW24 (20 nm for LW24) compared with the other porphyrins (17, 16, and 17 nm for LD14, LW4, and LW5) indicates a strong dipole moment in the excited states of this porphyrin.¹⁵ The bathochromic shift as well as broader PL spectra is an indication of intense charge transfer character within LW24 porphyrins' excited state. This will be discussed below.

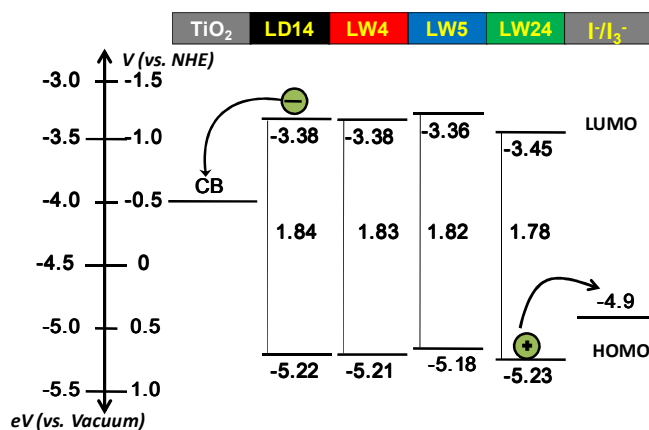


Fig. 3 Energy diagram of the sensitizers LD14, LW4, LW5, LW24, redox couple, and the conduction band of TiO_2 . The HOMO and LUMO levels were obtained from the ground state redox potentials and the optical energies. And the difference of the potential for the NHE (U_{redox}) versus an electron in vacuum ($E_{\text{F,redox}}$) can be given as: $E_{\text{F,redox}} [\text{eV}] = -4.5 - eU_{\text{redox}} [\text{V}]$.¹⁶

Table 1. Absorption, fluorescence, and first porphyrin-ring redox potential of various porphyrins (LD14, LW4, LW5 and LW24) in THF at 25 °C.

Dye	Absorption $\lambda_{\text{max}}^{[a]}$ / nm ($10^4 \text{ M}^{-1} \text{ cm}^{-1}$)	Emission $\lambda_{\text{max}}^{[b]}$ / nm	PL ^[c] lifetime τ /ns	$E_{\text{ox}}^{[c]}/\text{V}$ (vs. NHE)	$E_{0,0}^{[d]}/\text{V}$ (vs. NHE)	$E_{\text{ox}}-E_{0,0}$ /V
LD14 ^[f]	459(253.8) 667(64.1)	684	1.69	0.72	1.84	-1.12
LW4	462(234.1) 671(56.4)	687	1.54	0.71	1.83	-1.12
LW5	466(283.1) 674 (65.9)	691	1.66	0.68	1.82	-1.14
LW24	464(177.6) 689(87.8)	710	0.89	0.73	1.78	-1.05

[a] Absorption and emission data were measured in THF at 25 °C; [b] Excitation wavelength/nm: LD14, 459; LW4, 462; LW5, 466; LW24, 464; [c] First porphyrin ring oxidation; Electrochemical measurements were performed at 25 °C with each porphyrin (0.5 mM) in THF/0.1 M TBAP/ N_2 , GC working and Pt counter electrodes, Ag/AgCl reference electrode, scan rate=50 mV s^{-1} ; [d] Estimated from the intersection wavelengths of the normalized UV-vis absorption and the fluorescence spectra; [e] The

fluorescence time were measured under a laser excitation of 445 nm; [f] LD14 was synthesized according to the literature ref. 13.

The HOMOs calculated from their first oxidation potentials (E_{ox}) are determined to be -5.22, -5.21, -5.18 and -5.23 eV, while the LUMOs are -3.38, -3.38, -3.36 and -3.45 eV, if we transform the cyclic voltammetry (CV) to energy level in vacuum.¹⁶ The HOMO and LUMO values of the LD14 and LW4 porphyrins are identical, while difference in LW5 and LW24 is clearly indicated. It appears that the electron-deficient aromatic unit of BTD shifts the LUMO level negatively, while the electron-rich of thiophene unit mainly plays influence on the HOMO level. The distribution for HOMO and LUMO energy levels in such D-A structured porphyrin molecules are largely localized on the donor moiety and the acceptor moiety, respectively.¹⁷ In this case, the variation of energy levels could be explained by assuming the BTD unit serving as auxiliary acceptor in LW24, while thiophene serving as auxiliary donor in LW5. As depicted in Fig. 3, the conduction band of the TiO_2 locates at -4.0 eV, while the redox potential of the electrolyte is -4.9 eV.¹⁶ Thus these porphyrins are sufficient to ascertain the injection and regeneration reaction from a thermodynamic point of view (Fig. 2). Density-functional theory (DFT) calculations were also performed on the LD14 and LW4 dyes to gain insight into the electronic structures of their frontier molecular orbitals. As shown in Fig. S5, the HOMOs are localized on the donor (dimethylamine) and macrocycle moieties; in contrast, the LUMOs are highly visible on the macrocycle and the acceptor moieties (π -spacer and carboxyl acid).

Utilizing time-correlated single photon counting technique, we measured the fluorescence decay lifetime of LD14, LW4, LW5 and LW24 dyes, getting insight into the electron injection process from the photoexcited porphyrin to the TiO_2 conduction band.¹⁸ Fig. 4 presents the fluorescence decay for the porphyrin dyes in THF and on nanocrystalline TiO_2 films in the presence of electrolytes used in the photovoltaic experiments. In THF solution, the lifetime of the LD14, LW4, LW5 and LW24 dyes is 1.69, 1.54, 1.66 and 0.89 ns (in Table 1). The LW24 porphyrin shows the fastest decay among the tested samples, being nearly half of the other three porphyrins. It confirms a strong electron-coupling of the donor and acceptor in the excited state.¹⁹ When those porphyrins adsorbed onto the TiO_2 nanoparticles surface, a strong quenching of emission was observed. The lifetime of the excited singlet state of LD14, LW4, LW5 and LW24 and LD14 dyes in the adsorbed state is estimated to about 150 ps. This confirms a rapid electron injection from the excited state of sensitizers into the TiO_2 conduction band.²⁰

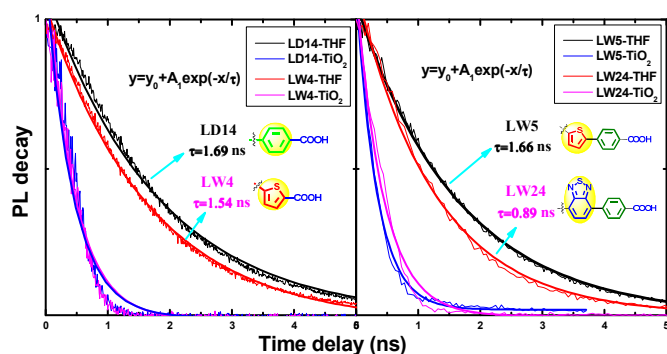


Fig 4. Time-resolved photoluminescence decay traces of dye-grafted mesoporous titania film and dye in THF solvent. Excitation wavelength: 445 nm, detected at: LD14, 684 nm; LW4, 687 nm; LW5, 691 nm; LW24, 710 nm. The traces with scatter are raw data; the solid curves are the results fitted according to the equation.

Nanosecond transient absorption spectrum were performed to scrutinize the dynamics of the recombination of electrons injected in the conduction band of $TiO_2(e_{cb})$ with the oxidized dye (S^+) and that of the dye regeneration reaction with iodide.²¹ Fig. 5 shows the transients at 550 nm for with the samples on titania in the presence and absence of the redox complex. The pump pulses at 460 nm are attenuated with neutral density filters before excitation of the sample with a fluence less than $40 \mu J cm^{-2}$. The decays have been fitted by a stretched-exponential function eq(1) as follows:²¹

$$A(t) = A_n e^{-(t/\tau)^\beta} \quad \text{eq(1)}$$

where τ is the characteristic lifetime, β being the stretch parameter ($0 < \beta < 1$, $\beta = 1$ corresponding to a monoexponential decay). The eq(1) takes account of the exponential distribution of energy states in the conduction band, the presence of trap states, and the different dye distributions onto the semiconductor surface.^{21b} In the devices containing solely inert electrolytes without redox couple, the electron recombination reaction is only on the interactions between the dye and the electrons located in the conduction band and the trap states of TiO_2 . Thus, the extracted lifetimes of LD14, LW4, LW5 and LW24 was estimated to be 56, 38, 8.8 and 11.4 ms as listed in Table 2. In the presence of redox couple, the oxidized dye molecules are not only reduced by the recombination process, but also the regeneration process via the electrolyte as well. In this case, the acquired lifetimes of LD14, LW4, LW5 and LW24 are 31, 35, 42 and 52 μs . To investigate the non-exponential decay analysis precisely, the average time constants and averaged rate are calculated according to the literature.^{21a-b}

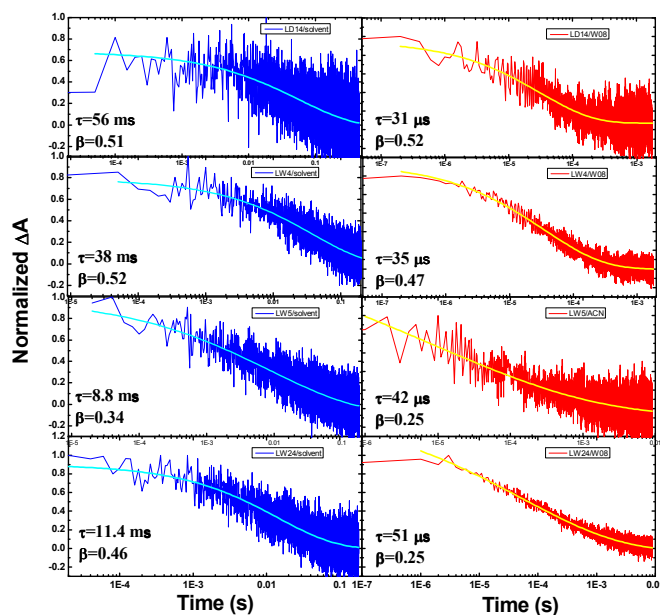


Fig. 5 Transient absorption spectra (TAS) of LD14, LW4, LW5, and LW24 porphyrins on mesoporous TiO₂, with or without redox couple (iodine based electrolyte, coded W08). The traces with scatter are raw data; the solid curves are the results fitted according to the equation. Excitation wavelength: 460 nm; detection wavelength: 550 nm.

Table 2. Parameters of the stretched exponential function used in the fit of the transient absorption signals for various porphyrins (LW4, LW5, LW24 and LD14) on TiO₂ electrode in the presence and absence of iodine-based electrolyte. Excitation wavelength is 460 nm and the detective wavelength is 550 nm. τ_1 and β are the parameters acquired from eq(1), τ_{obs} is the averaged time constant, k_{rec} and k_{reg} are the rate constant of recombination and regeneration process, respectively. ϕ_{reg} is the quantum yield of the dye regeneration.

dye	ACN			Γ/Γ_3^-			k_{rec} s ⁻¹	k_{reg} (M ⁻¹ s ⁻¹)	ϕ_{reg} (%)
	τ_1 (ms)	B	τ_{obs} (ms)	τ_1 (μ s)	β	τ_{obs} (μ s)			
LD14	56	0.5	108	31	0.5	70	9.3	4.7×10^5	99.9
LW4	38	0.5	71	35	0.4	79	14.1	4.2×10^5	99.9
LW5	8.8	0.3	23	42	0.2	10	43.5	2.9×10^4	95.6
LW24	11.4	0.4	27	51	0.2	12	37.0	2.4×10^4	95.5

In this configuration, the rate constant (k_{rec}) for recombination process calculated from the inverse of the recombination average time constants are 9.3, 14.1, 43.5 and 37.0 s⁻¹ for LD14, LW4, LW5 and LW24, respectively. Thus, the regeneration rate constant, k_{reg} , can be obtained by using eq(2) with the previously calculated value k_{rec} for the recombination:

$$k_{\text{reg}} = \frac{k_{\text{obs}} - k_{\text{rec}}}{[I^-]} \quad \text{eq(2)}$$

where the $[I^-]$ refers to the concentration of the reduced species of the redox pair. The k_{reg} calculated from eq(2) are 4.7×10^5 , 4.2×10^5 , 2.9×10^4 and 2.4×10^4 s⁻¹. The obviously slower oxidized dye regeneration rate of LW5 and LW24 could be explained by the longer conjugation length of molecules. Considering the different results from PL decay and TAS, it suggested different charge transfer processes from porphyrin sensitizers to semiconductor or to reduction species in the presence of electrolyte. Table 2 gives the obtained rate constants for the cells sensitized with LD14, LW4, LW5 and LW24. Finally, the quantum yield of the dye regeneration (ϕ_{reg}) for the complete device is determined from eq(3):²¹

$$\phi(\text{reg}) = \frac{k_{\text{reg}}[I^-]}{k_{\text{obs}}} \quad \text{eq(3)}$$

As showed in Table 2, the oxidized dye regeneration efficiencies are 99.9%, 99.9%, 95.6% and 95.5% for LD14, LW4, LW5 and LW24 devices, respectively. It is worth to note that the porphyrins (LW5 and LW24) featuring with longer π spacer (thiophene-phenyl or BTD-phenyl) exhibit slightly lower value of regeneration efficiency than that having shorter ones (phenyl or thiophene).

The driving force of the regeneration reaction can be informed from the difference of the electrolyte's redox potential and the dye's HOMO level. As illustrated in Fig. 3, it is evaluated to be similar driving force values of 0.32, 0.31, 0.28, and 0.33 eV for the LD14, LW4, LW5, and LW24, respectively. Therefore, we can conclude that the variation in ϕ_{reg} is not induced by the thermodynamic driving force.²² Generally, regeneration of the oxidized dye in homogeneous medium can be reasonably well described by the classic theory of electron transfer developed by Marcus.^{21c} Within this context, all the investigated porphyrins are designed with the same donor and porphinate group. We may ascribe the different rate of electron transfer between donor and acceptor to the variation of the conjugation length and intrinsic property of the spacer. As presented in Table 2, it is likely that an identical ϕ_{reg} could be found for these dyes possessing with similar conjugation length as evidenced in LW5 and LW24, or LD14 and LW4. Furthermore, the result infers that conjugation length plays critical influence onto the regeneration reaction in porphyrin based DSSC systems, rather than their intrinsic properties of those units. Thus, the regeneration is quite similar for the four samples regardless of electron-deficient or rich unit inserted between the porphine and benzoic acid.

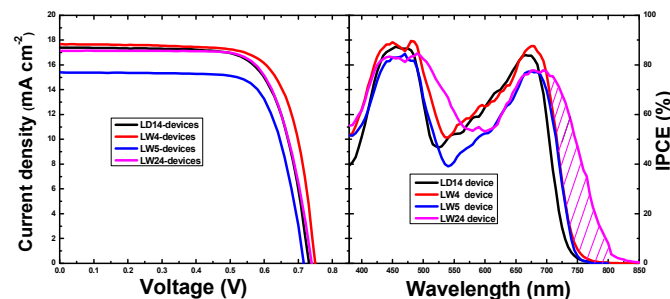


Fig. 6 a) J-V curves of and the DSSC devices based on LD14, LW4, LW5, and LW24 porphyrins measured under simulated AM 1.5G full sunlight; b) IPCE spectra of LD14, LW4, LW5, and LW24 porphyrins devices. The cells were measured with a mask (area=0.09 cm²).

By using an optimized binary solvent of toluene and ethanol (volume ratio 1:1), the porphyrins were sensitized onto a bilayer (7.5 + 5.0 μ m) titania film to serve as a working electrode. We evaluated these porphyrins in DSSC devices in combination with iodine-based electrolyte. The current-voltage (J-V) characteristics and the corresponding action spectra of incident photons to electrons conversion efficiency (IPCE) of the devices are shown in Fig. 6a and 6b. The photovoltaic parameters, i.e., PCE, short circuit photocurrent density (J_{SC}), the open circuit photovoltage (V_{OC}), and fill factor (FF) extracted from Fig. 6a are summarized in Table 3. The LD14 devices show a PCE 9.01% with a V_{OC} 734 mV, while LW4 devices exhibit 9.53% with a superior V_{OC} of 751 mV. The better performance of the latter is mainly benefited from the higher V_{OC} . However, for LW5, the J_{SC} of the corresponding devices decrease nearly 2 mA cm⁻², in spite of an enhanced light-harvesting ability around 725-750 nm. For the LW24 featured with BTD extended spacer, the IPCE tail of the corresponded devices significantly broadens to nearly 840 nm. Thus, the LW24 DSSC devices achieve a J_{SC} of 17.14 mA cm⁻². LW24 devices not only show higher PCE than LW5 devices, but also superior than LD14. The IPCE intensity is a

function of charge collection, electron injection in the TiO₂, and dye regeneration efficiency.²² As discussed above, the oxidized dye regeneration efficiencies of LW5 or LW24 are lower than LD14 or LW4, which may give a clue for the lower IPCE values in the former two kinds devices.

Table 3. Photovoltaic parameters (with standard deviations) of DSSC devices using LD14, LW4, LW5, and LW24 dyes in combination with iodine-based electrolyte under an irradiation at 100 mW cm⁻². Five independent cells were measured to obtain the average values. The cells were measured using a mask (area= 0.09 cm⁻²).

Device	J _{sc} (mA cm ⁻²)	V _{OC} (V)	FF	PCE(%)
LD14	17.38±0.10	0.734±0.006	0.710±0.002	9.01±0.06
LW4	17.65±0.18	0.751±0.008	0.720±0.003	9.53±0.07
LW5	15.41±0.12	0.719±0.004	0.735±0.005	8.16±0.10
LW24	17.14±0.20	0.737±0.012	0.723±0.012	9.21±0.12

The V_{OC} is defined as the energy difference between the quasi-Fermi level (E_F) of the TiO₂ under illumination and the Nernst potential of the redox electrolyte (E_{F,redox}).²² Since all the devices here utilize similar electrolytes, TiO₂ photoanode and fabrication processes, the variations of V_{OC} can be rationalized explained based on the changes of electronic E_F, which depends on the electron density in the TiO₂.²³ In this case, we performed transient photovoltage decay and charge extraction measurements to understand the physical origin of the V_{OC} difference between the four porphyrins based DSSC.²⁴ Fig. 7a presents the capacitance (C_μ) at different voltages for various DSSC. The C_μ follows the expression of C_μ ∝ exp(qV/mkT),²⁵ where *k* is the Boltzmann constant, *T* is the absolute temperature, and *m* is related to the shape of the distribution of the density of states. Similar slopes for the plots in Fig. 7a indicate the same trap state distribution in the TiO₂ for various devices. At the identical C_μ, the open-circuit voltage of the LW24 device is about 10-20 mV higher than the other devices (Fig.7a). Whilst the LD14 devices show a slight 5 mV lower than LW4 and LW5 devices, and 15 mV lower than LW24. Sensitizers adsorbed on the semiconductor surface can modify its electronic properties, such as band bending, on account of different dipole moments (Δφ ∝ Nμcosθ, where Δφ is the electrostatic potential drop, N being the number of adsorbed molecules per surface area, μ being the molecular dipole moment, θ being the tilt angle between the axes of the dipole moment and the surface normal of the TiO₂ particles). Neglecting the amount and tilt angle of the four porphyrins adsorbed on TiO₂,²⁷ it is likely that the higher TiO₂ band bending edge in LW24 devices could be explained by the bigger dipole moment of LW24 porphyrin. Fig. 7b presents the electron lifetime (τ) as a function of electron density, which further provides the information about recombination between the injected electrons in the TiO₂ and the oxidized form of electrolytes.³ All devices showed similar shape of the curves in Fig. 7b, which may be ascribed to the efficient insulation of the TiO₂ surface by the same four dodecyloxy-chains.²⁸ At a given electron density, the electron lifetime of LW4 device is longer than the other three porphyrins, while the LW24 device is the shortest one. The BT

group can accelerate conduction-band electron recapture by the sensitizer.^{3b,3c,7} Thus, we ascribe the lower V_{OC} of the LW24 in comparison with LW4 devices to a serious recombination reaction.

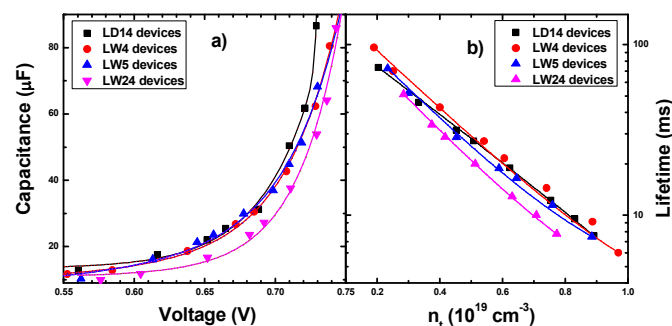


Fig. 7 Transient photovoltage decay and charge extraction measurements of LD14, LW4, LW5, and LW24 based DSSC devices. a) Comparisons of chemical capacitance at a certain open-circuit photovoltage; b) Comparisons of electron lifetime at a given electron density.

Conclusions

In summary, we have shown a systematic investigation of the influence from varied π-spacers in porphyrin sensitizers on the photo-induced charge transfer processes and photovoltaic performance. The results reveal the electron-deficient unit BTB inserted between porphyrin core and the benzoic acid anchoring group could lead to a broadened light-harvesting spectral region as well as an upward shift of the conduction band edge of TiO₂. However, the electron-rich unit thiophene at the same site shows less significant impact. These results could be explained by the difference of electron coupling in the excited state as well as internal charge transfer within the molecule. Porphyrins with solely aromatic spacer shows prolonged electron lifetime and faster dye-regeneration reaction in comparison with the spacer extended porphyrins. The compromised effect brought about by the extension of the conjugation length results in the overall conversion efficiency of 9.2% for LW24, while LW4 with shorter spacer presented the highest efficiency of 9.5%. We believe that this structure–property relationship will shed light on a better molecular design and synthesis of panchromatic porphyrin sensitizers to further improve the photovoltaic performance for a DSSC.

Acknowledgements

JL, HL, SL, YC, and MW thank the Director Fund of WNLO, the 973 Program of China (2014CB643506 and 2013CB922104) and NSFC (21173091) for financial support; they also thank the Analytical and Testing Centre at HUST for performing characterization of various samples. YCC, HPW and EWGD received support from National Chiao Tung University (NCTU), Ministry of Science and Technology (MOST) of Taiwan and Ministry of Education (MOE) of Taiwan. The authors also thank Prof. Jie Xu for the DFT calculation results. JL thanks NCTU (Hsinchu, Taiwan) and WNLO (Wuhan, China) for supporting of his visit to NCTU.

Notes and references

^a Wuhan National Laboratory for Optoelectronics, School of Optical and Electronic Information, Huazhong University of Science and Technology, 1037 Luoyu Road, Wuhan 430074, P. R. China, Fax: (+) 86-27-87792225, mingkui.wang@mail.hust.edu.cn.

^b Department of Applied Chemistry and Institute of Molecular Science, National Chiao Tung University, Hsinchu 30010, Taiwan, Fax:+886-3-5723764; Tel:+886-3-5131524; E-mail: diau@mail.nctu.edu.tw.

^c Department of Materials Engineering, Monash University, Melbourne, Victoria, 3800, Australia.

‡ Notes: J. Lu and H. Li contributed equally.

† Electronic Supplementary Information (ESI) available: [details of any supplementary information available should be included here]. See DOI: 10.1039/b000000x/

- 1 T. Hasobe, H. Imahori, P. Kamat, T. Ahn, S. Kim, D. Kim, A. Fujimoto, T. Hirakawa and S. Fukuzumi, *J. Am. Chem. Soc.*, 2005, **127**, 1216–1228.
- 2 a) H. Imahori, T. Umeyama and S. Ito, *Acc. Chem. Res.*, 2009, **42**, 1809–1818; b) L.-L. Li and E. W.-G. Diau, *Chem. Soc. Rev.* 2013, **42**, 291–304; c) M. Urbani, M. Grätzel, M. K. Nazeeruddin and T. Torres, *Chem. Rev.* 2014, **114**, 12330–12296; d) T. Higashino and H. Imahori, *Dalton Trans.*, 2015, **44**, 448–463; e) J. Kesters, P. Verstappen, M. Kelchtermans, L. Lutsen, D. Vanderzande and W. Maes, *Adv. Energy Mater.* 2015, **5**, 1500218; f) D. Huang, J. Lu, S. Li, Y. Luo, C. Zhao, B. Hu, M. Wang and Yan Shen, *Langmuir*, 2014, **30**, 6990–6998.
- 3 a) T. Bessho, S. Zakeeruddin, C.-Y. Yeh, E. W.-G. Diau and M. Grätzel, *Angew. Chem. Int. Ed.*, 2010, **49**, 6646–6649; b) A. Yella, H. Lee, H. Tsao, C. Yi, A. Chandiran, M. Nazeeruddin, E. W.-G. Diau, C.-Y. Yeh, S. Zakeeruddin and M. Grätzel, *Science*, 2011, **334**, 629–634; c) M. Mathew, A. Yella, P. Humphry-Baker, B. Curchod, N. Ashari-Astani, I. Tavernelli, U. Rothlisberger, M. Nazeeruddin, M. Grätzel, *Nat. Chem.*, 2014, **6**, 242–247; d) Y. Xie, Y. Tang, W. Wu, Y. Wang, J. Liu, X. Li, H. Tian and W. Zhu, *J. Am. Chem. Soc.*, 2015, **137**, 14055–14058; e) C.-L. Wang, M. Zhang, Y.-H. Hsiao, C.-K. Tseng, C.-L. Liu, M. Xu, P. Wang, C.-Y. Lin, *Energy Environ. Sci.*, 2015, DOI: 10.1039/C5EE02505B.
- 4 a) C.-W. Lee, H.-P. Lu, C.-M. Lan, Y.-L. Huang, Y.-R. Liang, W.-N. Yen, Y.-C. Liu, Y.-S. Lin, E. W.-G. Diau and C.-Y. Yeh, *Chem. – Eur. J.*, 2009, **15**, 1403–1412; b) W. Li, Z. Liu, H. Wu, Y. Cheng, Z. Zhao, and H. He, *J. Phys. Chem. C*, 2015, **119**, 5265–5273; c) W. Li, L. Si, Z. Liu, Z. Zhao, H. He, K. Zhu, B. Moore, and Y. Cheng, *J. Mater. Chem. A*, 2014, **2**, 13667–13674.
- 5 a) K. Kurotobi, Y. Toude, K. Kawamoto, Y. Fujimori, S. Ito, P. Chabera, V. Sundström and H. Imahori, *Chem. – Eur. J.*, 2013, **19**, 17075–17081; b) M. Ishida, D. Hwang, Z. Zhang, Y. Choi, J. Oh, V. Lynch, D. Kim, J. Sessler and D. Kim, *ChemSusChem*, 2015, **8**, 2967–2977; c) Y. Wang, B. Chen, W. Wu, X. Li, W. Zhu, H. Tian and Y. Xie, *Angew. Chem. Int. Ed.*, 2014, **53**, 10779–10783; d) F. Jradi, D. O'Neil, X. Kang, J. Wong, P. Szymanski, T. Parker, H. Anderson, M. El-Sayed and S. Marder, *Chem. Mater.*, 2015, **27**, 6305–6313.
- 6 a) K. Ladomenou, T. Kitsopoulos, G. Sharma and A. Coutsolelos, *RSC Adv.*, 2014, **4**, 21379–21404; b) M. Sreenivasu, A. Suzuki, M. Adachi, C. Kumar, B. Srikanth, S. Rajendar, D. Rambabu, R. Kumar, P. Malleshm, N. Bhaskar Rao, M. Kumar and P. Reddy, *Chem. – Eur. J.*, 2014, **20**, 14074–14083.
- 7 A. Yella, C.-L. Mai, S. Zakeeruddin, S.-N. Chang, C.-H. Hsieh, C.-Y. Yeh and M. Grätzel, *Angew. Chem., Int. Ed.*, 2014, **126**, 3017–3021.
- 8 L. Cabau, C. Kumar, A. Moncho, J. Clifford, N. López, and E. Palomares, *Energy Environ. Sci.*, 2015, **8**, 1368–1375.
- 9 H. Salm, S. Lind, M. Griffith, P. Wagner, G. Wallace, D. Officer and K. Gordon, *J. Phys. Chem. C*, 2015, **119**, 22379–22391.
- 10 S. Fan, K. Lv, H. Sun, G. Zhou and Z. Wang, *J. Power Sources*, 2015, **279**, 36–47.
- 11 a) C.-H. Wu, M.-C. Chen, P.-C. Su, H.-H. Kuo, C.-L. Wang, C.-Y. Lu, C.-H. Tsai, C.-C. Wu and C.-Y. Lin, *J. Mater. Chem. A*, 2014, **2**, 991–999; b) J. Luo, M. F. Xu, R. Z. Li, K. W. Huang, C. Y. Jiang, Q. B. Qi, W. D. Zeng, J. Zhang, C. Y. Chi, P. Wang, J. S. Wu, *J. Am. Chem. Soc.*, 2014, **136**, 265–272; c) Q. Qi, R. Li, J. Luo, B. Zhang, K. Huang, P. Wang, W. Wu, *Dyes Pigments*, 2015, **122**, 199–205; d) J.-W. Shiu, Y.-C. Chang, C.-Y. Chan, H.-P. Wu, H.-Y. Hsu, C.-L. Wang, C.-Y. Lin and E. W.-G. Diau, *J. Mater. Chem. A*, 2015, **3**, 1417–1420.
- 12 a) J. Lu, X. Xu, K. Cao, J. Cui, Y. Zhang, Y. Shen, X. Shi, L. Liao, Y. Cheng and M. Wang, *J. Mater. Chem. A*, 2013, **1**, 10008–10015; b) J. Lu, B. Zhang, S. Liu, H. Yuan, Y. Shen, Y. Cheng, J. Xu and M. Wang, *Phys. Chem. Chem. Phys.*, 2014, **16**, 24755–24762; c) J. Lu, S. Liu, H. Li, Y. Shen, Y. Cheng, J. Xu and M. Wang, *J. Mater. Chem. A*, 2014, **2**, 17495–17501; d) J. Lu, B. Zhang, H. Yuan, X. Xu, K. Cao, J. Cui, S. Liu, Y. Shen, Y. Cheng, J. Xu and M. Wang, *J. Phys. Chem. C*, 2014, **118**, 14739–14748; e) J. Lu, Y.-C. Chang, H.-Y. Cheng, H.-P. Wu, Y. Cheng, M. Wang, and E. W.-G. Diau, *ChemSusChem*, 2015, **8**, 2529–2536.
- 13 Y.-C. Chang, C.-L. Wang, T.-Y. Pan, S.-H. Hong, C.-M. Lan, H.-H. Kuo, C.-F. Lo, H.-Y. Hsu, C.-Y. Lin and E. W.-G. Diau, *Chem. Comm.*, 2011, **47**, 8910–8912.
- 14 a) J. Lu, X. Xu, Z. Li, K. Cao, J. Cui, Y. Zhang, Y. Shen, Y. Li, J. Zhu, S. Dai, W. Chen, Y. Cheng and M. Wang, *Chem. – Asian J.*, 2013, **8**, 956–962; b) J. Lu, S. Liu, Y. Shen, J. Xu, Y. Cheng and M. Wang, *Electrochimica Acta*, 2015, **179**, 187–196.
- 15 S. Haid, M. Marszalek, A. Mishra, M. Wielopolski, J. Teuscher, J. Moser, R. Humphry-Baker, S. Zakeeruddin, M. Grätzel and P. Bäuerle, *Adv. Funct. Mater.*, 2012, **22**, 1291–1302.
- 16 a) M. Grätzel, *Nature*, 2001, **414**, 338–344; b) A. Hagfeldt, G. Boschloo, L. Sun, K. Kloo and H. Pettersson, *Chem. Rev.* 2010, **114**, 6595–6663; c) M. Wang, C. Grätzel, S. Zakeeruddin and M. Grätzel, *Energy Environ. Sci.*, 2012, **5**, 9394–9405.
- 17 a) X. Gu and Q. Sun, *Phys. Chem. Chem. Phys.*, 2013, **15**, 15434–15440; b) T. Wei, X. Sun, X. Li, H. Ågren and Y. Xie, *ACS Appl. Mater. Interfaces*, 2015, **7**, 21956–21965.
- 18 a) R. Katoh and A. Furube, *J. Photochem Photobiol C Photochem Rev.*, 2014, **20**, 1–16; b) R. Milot and C. Schmittenmaer, *Acc. Chem. Res.*, 2015, **48**, 1423–1431.
- 19 A. Margalias, K. Seintis, M. Yigit, M. Can, D. Sygkridou, V. Giannetas, M. Fakis and E. Stathatos, *Dyes Pigments*, 2015, **121**, 316–327.
- 20 L.-Y. Luo, R. Ambre, S. Mane, E. Diau and C. Hung, *Phys. Chem. Chem. Phys.*, 2015, **17**, 20134–20143.
- 21 a) A. Anderson, P. Barnes, J. Durrant and B. O'Regan, *J. Phys. Chem. C*, 2011, **115**, 2439–2447; b) P. Piatkowski, C. Martin, M. Nunzio, B. Cohen, S. Pandey, S. Hayse and S. Douhal, *J. Phys. Chem. C*, 2014, **118**, 29674–29687; c) S. Feldt, G. Wang, G. Boschloo and H. Hagfeldt, *J. Phys. Chem. C*, 2011, **115**, 21500–21507.
- 22 A. Yella, R. Humphry-Baker, B. Curchod, N. Astani, J. Teuscher, L. Polander, S. Mathew, J. Moser, I. Tavernelli, U. Rothlisberger, M.

- Grätzel, M. Nazeeruddin and J. Frey, *Chem. Mater.*, 2013, **25**, 2733–2739.
- 23 A. Reynal, A. Forneli, E. Martinez-Ferrero, A. Sanchez-Diaz, A. Vidal-Ferran, B. O'Regan, E. Palomares, *J. Am. Chem. Soc.*, 2008, **130**, 13558–13567.
- 24 a) L.-L. Li, Y.-C. Chang, H.-P. Wu and E. W.-G. Diau *Int. Rev. Phys. Chem.*, 2012, **31**, 420–467; b) M. Griffith,; K. Sunahara, P. Wagner, K. Wagner, G. Wallace, D. Officer, A. Furube, R. Katoh, S. Mori and A. Mozer, *Chem. Commun.*, 2012, **48**, 4145–4162.
- 25 S. Jang, K. Zhu, M. Ko, K. Kim, C. Kim, N. Park and A. Frank, *ACS Nano*, 2011, **5**, 8267–8274.
- 26 S. Rühle, M. Greenshtein, S. Chen, A. Merson, H. Pizem, C. Sukenik, D. Cahen and A. Zaban, *J. Phys. Chem. B*, 2005, **109**, 18907–18913.
- 27 a) S. Ye, A. Kathiravan, H. Hayashi, Y. J. Tong, Y. Infahsaeng, P. Chabera, T. Pascher, A. Yartsev, S. Isoda, H. Imahori and V. Sundström, *J. Phys. Chem. C*, 2013, **117**, 6066–6080; b) H. Hayashi, T. Higashino, Y. Kinjo, Y. Fujimori, K. Kurotobi, P. Chabera, V. Sundström, S. Isoda and H. Imahori, *ACS Appl. Mater. Interfaces*, 2015, **7**, 18689–18696.
- 28 C.-L. Wang, J.-Y. Hu, C.-H. Wu, H.-H. Kuo, Y.-C. Chang, Z.-J. Lan, H.-P. Wu, E. W.-G. Diau and C.-Y. Lin, *Energy. Environ. Sci.*, 2014, **7**, 1392–1396.

Novel porphyrins – preparation, characterization, and application in solar energy conversion

By: J. Lu, H. Li, S. Liu, Y. Chang, H. Wu, Y. Cheng, E. Diau, and M. Wang

Accelerated inner charge transfer in porphyrin promotes broad light-harvesting ability up to 840 nm and a conversion efficiency of 9.2%.

